




Demand Response Program Integrated With Electrical Energy Storage Systems for Residential Consumers

Motahar Tehrani, *Student Member, IEEE*, Mehrdad Setayesh Nazar , *Member, IEEE*, Miadreza Shafie-khah , *Senior Member, IEEE*, and João P. S. Catalão , *Fellow, IEEE*

Abstract—This article presents a distributed resilient demand response program integrated with electrical energy storage systems for residential consumers to maximize their comfort level. A dynamic real-time pricing method is proposed to determine the hourly electricity prices and schedule the electricity consumption of smart home appliances and energy storage systems commitment. The algorithm is employed in normal and emergency operating conditions, taking into account the comfort level of consumers. In emergency conditions, the power outage of consumers is modeled for different hours and outage patterns. To evaluate the applicability of the proposed model, real samples of Southern California households are considered to model the smart homes and their appliances. Further, a sensitivity analysis is performed to assess the impacts of the number of households and number of persons per household on the output results. The results showed that the proposed model reduced the costs of utility in normal and emergency conditions by about 33.77% and 30.92%, respectively. The values of total payments of consumers in normal and emergency conditions were decreased by about 34.26% and 31.31%, respectively. Further, the consumers comfort level for normal and emergency conditions increased by about 146.78% and 110.2%, respectively. Finally, the social welfare for normal and emergency conditions increased by about 46% and 49.06%, respectively.

Index Terms—Building automation, demand-side management, optimization, smart grid, smart homes.

I. INTRODUCTION

SMART home is a new conceptual framework and technical tool to enhance the resiliency of electrical system consumers. Most electric utilities have been designed in a way to withstand stochastic outages of electrical equipment under the $N-1$ security criteria [1]. However, natural disasters, human errors, and terrorist attacks have posed unprecedented challenges

Manuscript received February 21, 2021; revised September 24, 2021; accepted January 30, 2022. The work of João P. S. Catalão was supported in part by FEDER funds through COMPETE 2020 and in part by the Portuguese funds through FCT under Grant POCI-010145-FEDER-029803 (02/SAICT/2017). (Corresponding authors: Miadreza Shafie-khah; João P.S. Catalão.)

Motahar Tehrani and Mehrdad Setayesh Nazar are with the Shahid Beheshti University, Tehran 19839 69411, Iran (e-mail: tehranitata@yahoo.com.; setayeshnazar@yahoo.com.).

Miadreza Shafie-khah is with the School of Technology and Innovations, University of Vaasa, 65200 Vaasa, Finland (e-mail: miadreza@gmail.com).

João P. S. Catalão is with the Faculty of Engineering of University of Porto, and INESC TEC, 4099-002 Porto, Portugal (e-mail: catalao@ubi.pt).

Digital Object Identifier 10.1109/JSYST.2022.3148536

to electrical supply systems and smart home planning and operational methods are introduced to reduce the impacts of these external shocks.

A resilient electrical system should withstand severe disturbances without experiencing any major electricity disruption, enable quick recovery, and restore to the normal operating state [2]. Smart home energy management systems (SHEMSs) can be utilized to increase the resiliency of consumers and manage their energy consumptions [3]. The SHEMS can reduce the impacts of the external shocks and households' dependency on the main grid using energy storage systems (ESSs) and distributed energy resources (DERs) [4].

Over the recent years, different aspects of resilient smart homes are presented and the literature can be categorized into the following three categories: electric vehicle commitment strategies in emergency conditions; load commitment strategies in emergency conditions; and combinations of the above strategies with DERs and ESSs commitment in emergency conditions.

Based on the above categorization and for the first category of papers, Abessi and Jadid [5] introduced the internal combustion engine vehicle as an electrical energy source in external shock conditions. The proposed method improved the resilience of the system by supplying the smart homes with internal combustion engine vehicles and injecting the extra electrical power of smart homes into the distribution system. However, the model did not consider the optimal load commitment of smart appliances in normal conditions and the real-time pricing process. Rahimi and Davoudi [6] proposed a process to supply residential consumers with plug-in electric vehicles (PHEVs) during external shocks. The model minimized the peak power of smart appliances that were supplied by electric vehicles. Different electricity consumption scenarios during seasons were simulated. The method did not model the comfort level of consumers and dynamic real-time pricing procedure. Razeghi *et al.* [7] assessed the impact of PHEVs on the resiliency of the system during its outages. The results showed that during normal operating conditions, the increased values of the electrical demand of PHEVs reduced the system resiliency by stressing system components. This process accelerated aging, increased the probability of failure, and reduced the reliability and resiliency of the system. However, the proposed model only considered the supplying of critical load during outages using PHEVs. Xu and Chung [8] evaluated the impacts of the vehicle to home and vehicle to grid operating

modes on the system reliability and results indicated that the reliability of the system with the vehicle to grid contributions was improved. The optimization process utilized a central charging algorithm for PHEVs in emergency conditions. The proposed framework did not supply the entire load. Further, the method did not model the comfort level of consumers.

For the second category of studies, Srikantha and Kundur [9] introduced a distributed demand response program (DRP) that curtailed loads and improved the resilience of the system. The model minimized the compensation costs of the system that were paid to consumers to reduce their energy consumptions. The framework did not consider the detailed model of smart appliances and the comfort level of consumers. Balasubramaniam *et al.* [10] assessed a resilient optimization model that utilized the adjustable loads to supply the critical loads in external shock conditions and increase the system resiliency. The process minimized the aggregated load shedding and maximized the served noncritical loads. However, the process did not assess the consumer comfort level. Nourollahi *et al.* [11] presented a robust optimization process to enhance the resiliency of the system using DRPs. The proposed model considered the uncertainties of external shocks, intermittent power generations, and load and price parameters. However, the method did not study the commitment scenarios of smart appliances of consumers. Liu *et al.* [12] assessed an optimization algorithm for utilizing the load curtailment process to increase the resiliency of the system in extreme conditions. The loss of load probability, expected demand not supplied, and grid recovery indices were utilized to optimize the recovery process of the system. The interactions of transmission, distribution, and microgrid systems were modeled. The curtailment process did not model the consumers comfort level and real-time pricing. Aghaei *et al.* [13] evaluated an emergency DRP process that was utilized to reduce the expected load not served in contingent conditions. The proposed model considered the dynamic elasticity of demand and minimized the system operating costs, incentive costs that were paid to consumers, and expected load not served costs. The optimization procedure did not utilize the real-time pricing process. Samarakoon *et al.* [14] proposed a load reduction algorithm based on local frequency measurement. The load control method aggregated typical domestic appliances, according to the maximum admissible time for disconnecting the loads without harming consumers' comfort. The load control process was carried out by smart meters to provide primary frequency response. The process did not formulate the commitment of smart appliances in normal conditions. Short *et al.* [15] developed a dynamic load control method that turned OFF refrigerators based on frequency and temperature without considering consumers comfort level. The proposed method improved the stability of the power system when facing a loss of generation, an increase in load, or high penetration of variable generation resources. Yu *et al.* [16] proposed a distributed energy management control process that utilized the load control/curtailment process to minimize the loss of load and reduce the peak-to-average demand ratio. The objective function maximized the social welfare compromised demand surplus minus utility costs. The energy management method did not study the real-time pricing models. Lu and Zhang [17] examined a central load control mechanism for thermostatically controlled

appliances to provide a continuous regulating reserve. The model considered the heating, ventilating, and air-conditioning loads and the results showed that the proposed method provided 24 h of intrahour continuous balancing services. However, the control strategy did not commit the smart home appliances in contingent conditions. Vivekananthan and Mishra [18] evaluated a stochastic ranking method to provide regulation services by retailers. The retailer participated in the day-ahead market and responded to the control signals of the real-time market. The stochastic behavior of temperature variation, status, and power consumption of loads was modeled by the Markov property. The procedure was centrally computed and the proposed model improved the resiliency of the system. Nevertheless, the ranking method was not able to model the consumers' comfort levels.

For the third category of studies, Mehrjerdi [1] introduced an optimization process for battery swapping and increasing the resiliency of buildings that were equipped with photovoltaic arrays, electric vehicles, and ESSs. The battery swapping process made the electric vehicle available for its owner at all times. The model minimized the operating cost of the integrated system considering the uncertainties of photovoltaic system electricity generation. The results presented that the reserve battery reduced the costs of the system by about 8%. However, the proposed method did not formulate the consumer comfort level in contingent conditions. Dinh and Kim [2] assessed an optimization framework for SHERMS that integrated ESS and DERs considering the comfort levels of consumers. The process minimized the installation costs of ESSs and DERs based on normal, economic, and smart modes of SHERMS operating scenarios. The results showed that the smart scenario reduced the energy cost of the system by about 46.4%. The introduced model did not examine the real-time pricing process and model the cost function of utility. Chatterji and Bazilian [3] presented a stochastic programming model to increase the resiliency of the system and minimize the cost of energy supply considering the photovoltaic system and ESSs. The model utilized the Monte Carlo simulation process to simulate the impacts of storm-related outages on the system. The emergency DRP was carried out to reduce the system cost and increase the resiliency of the system. The optimal load commitment of smart homes in the contingent scenario was not modeled. Mehrjerdi [4] assessed a model for resilient buildings that utilized electric vehicles and minimized the photovoltaic energy integration. The photovoltaic energy was used for daytime and the electric vehicle energy was available for nighttime using the adaptable charging-discharging process. The proposed method increased the resiliency of buildings and restored by about 51.5% of critical loads in contingent conditions. However, the algorithm did not encounter the real-time pricing and consumer comfort level. Rosales-Asensio *et al.* [19] evaluated the resiliency of the electrical system of large buildings integrated with photovoltaic arrays and electrochemical ESSs. The results showed that the resiliency of buildings was highly improved using the photovoltaic and energy storage facilities. Further, the designed system would be able to produce up to 49% of the total required energy. The model did not optimize the commitment process of smart homes in contingent conditions. Mehrjerdi and Hemmati [20] assessed an energy management system to minimize the operating cost of building and maximize

the resiliency of the system. The model considered energy hubs, distributed generations, and utilized the load shedding process in contingent conditions. The seasonal pattern for wind energy, loads, and prices were considered and the uncertainties of loads and wind energy generation were modeled. However, the framework did not formulate the consumer comfort level and real-time pricing process. Vahedipour-Dahraie *et al.* [21] proposed a stochastic risk-constrained optimization framework to maximize the expected profit of the system considering the demand and supply uncertainties. The conditional value-at-risk method was utilized to control nondesirable profits due to the system's uncertainties. The impacts of consumers' participation in DRPs on the values of lost load, conditional value-at-risk, and expected energy not supplied were investigated. The optimization model did not formulate the comfort level of consumers. Vahedipour-Dahraie *et al.* [22] introduced a risk-constrained stochastic framework for resilient operational scheduling of a system considering DRP. The optimization process minimized the system costs for normal and islanded operating modes. The value-at-risk metric was utilized to control the risk of profit variability. The framework did not utilize the real-time pricing procedure. Further, the implementation of mandatory load shedding programs reduced the consumers' comfort levels.

Tian and Talebizadehsardari [23] assessed the resiliency of buildings in extreme conditions considering the electric vehicles commitment, load adjustment, and load curtailment. The optimization algorithm minimized the building energy costs, load curtailment costs, and partial charge of electric vehicles. The load curtailment program shed the buildings' load up to 90% based on the fact that the process did not encounter the comfort level of consumers. Mehrjerdi *et al.* [24] examined the tradeoff between efficiency and resiliency of smart buildings. The building was equipped with energy management systems, ESS, photovoltaic arrays, and distributed generation. The proposed method minimized the investment and operating costs and maximized the resiliency of buildings. The model determined the minimum levels of nonrestored loads and utilized the load-shedding process. However, the method did not formulate the real-time pricing model and consumer comfort level. Gaikwad *et al.* [25] presented a predictive control process to commit the critical loads and ESSs. The optimization algorithm utilized mixed-integer linear programming to solve the formulated problem. The system was equipped with a photovoltaic array and ESS and the control method increased the resiliency of the system. The case study was carried out for a family house in Florida. However, the proposed model only supplied part of the loads during emergency conditions and did not study the comfort level of consumers. Gouveia *et al.* [26] assessed an online control process for improving the resiliency of islanded microgrids that utilized storage devices, PHEVs, and DRPs. The method controlled the loads to provide primary response frequency. The proposed methodology did not optimize the real-time pricing process. The introduced method shed the load to recover system frequency. Guo *et al.* [27] proposed a resilience-oriented stochastic optimization framework considering DRPs. The worst-case conditional value-at-risk theory was used to minimize the worst-case cost caused by an external shock. A

stochastic chance-constrained programming model was developed for the worst-case cost scenario. The proposed model increased the resiliency of the system by about 3.2%. The method did not examine the real-time pricing process. Hafiz *et al.* [28] introduced a distribution service restoration framework based on a multitime-step dynamic optimization model to achieve grid resiliency against natural disasters using DRPs. The proposed model utilized a three-step optimization procedure. In the first step, the method determined the aggregate controllable loads of the system. Then, at the second step, the candidate buses were selected. Finally, at the third step, the load control was performed using an energy management system. However, the model did not study the consumer comfort level and real-time pricing process. Eseye *et al.* [29] presented a two-stage algorithm for energy flexibility optimization of smart buildings for day-ahead and real-time markets. The proposed method considered PHEV, renewable energy electricity generation, ESS, and DRP. The model carried out DRP to improve the resiliency of the building. The process utilized load shedding/curtailment programs that reduced the comfort level of consumers.

Vahedipour-Dahraie *et al.* [30] introduced a risk-constrained stochastic optimization process to maximize the expected profit of a microgrid considering the uncertainties of price, load, and intermittent electricity generation. The tradeoffs between the risk of low profits in worst-case scenarios and system owner profits were modeled. The results presented that the participation of responsive loads increased the uncertainties of the system and more reserves were allocated for higher values of risk-aversion parameters. The procedure did not examine the real-time pricing model. Gholami *et al.* [31] assessed a stochastic programming model to schedule the energy resources of a resilient microgrid. The uncertainties of external shocks, market prices, electric vehicle commitments, and wind turbine electricity generations were modeled. The output results revealed that the proposed model increased the value of operating costs and decreased the expected load shedding costs. However, the model did not study the real-time pricing and load commitment process.

A framework that solves the optimal resilient DRP integrated with energy storage considering the consumers comfort levels in emergency conditions is less frequent in the literature. In this article, a distributed resilient DRP is proposed to improve the resiliency of smart homes in emergency conditions and maximize their comfort levels. The proposed DRP schedules the power consumptions of smart appliances and the charging/discharging power of electrical energy storage and utilizes a dynamic real-time pricing method.

The contributions of this article are as follows.

- 1) A dynamic real-time pricing method is proposed to determine the optimal values of hourly electricity prices and schedule the electricity consumption of smart home appliances and energy storage systems commitment.
- 2) The algorithm considers the interaction between SHERMSs, smart appliances, and the upward distribution system in normal and emergency operating conditions, taking into account the comfort level of consumers.
- 3) The proposed model immediately supplies the consumers' appliances after a power outage in the system without requiring external resources.

- 4) The optimization process determines the worst-case scenarios of operating conditions and in the case of emergency conditions; there is not any load shedding or curtailment program.
- 5) Real samples of Southern California households are used to model smart appliances and ESSs. The results indicate that the proposed distributed DRP method successfully reduced the distribution system and consumers costs and enhanced the resiliency of smart homes in both emergency and normal conditions.

The rest of this article is organized as follows. The proposed framework is formulated in Section II. In Section III, the solution algorithm is introduced. The simulation data is presented in Section IV and the simulation results of real samples are assessed in Section V. Finally, conclusion is presented in Section VI.

II. PROBLEM MODELING AND FORMULATION

It is assumed that a utility company supplies J residential consumers in the smart grid infrastructure. The simulation interval consists of 24 equal periods that t represent each of the simulation periods $t \in T = \{1, 2, \dots, 24\}$. The model of the utility company, residential consumers, SHEM, and ESS are presented in the following sections.

A. Model of Utility

The utility company minimizes the costs of energy purchased from the wholesale market. It is assumed that the utility company's cost function $\text{Cost}(p(t))$ is a convex function of p for time t , in which p is the active power that the utility purchases from the wholesale market. The utility company determines the optimal real-time energy prices ($\text{Pr}(t), t \in T$) by running a dynamic real-time pricing program at the beginning of each day in cooperation with the SHEMSs of households.

B. Model of Residential Consumers

Each consumer $i \in J$ has a set of smart home devices D , and $d \in D$ identifies each device. The power and energy consumption of device d that is owned by the consumer i at time t equal to $p_{i,d}(t)$ and $E_{i,d}$, respectively. The $\text{Wel}_{i,d}(p_{i,d}(t))$ is the welfare of the consumer i that he/she derives from using appliance d at time t . In other words, $\text{Wel}_{i,d}(p_{i,d}(t))$ equals cost of electricity consumption that the consumer i pays to the utility for using the device d at time t . Thus, the higher value of $\text{Wel}_{i,d}(p_{i,d}(t))$ corresponds to the higher value of the comfort level of the consumer i . Hence, CL_i can be defined as the comfort level of consumer i that equals the net welfare of the consumer. The net welfare of the consumer equals the gross welfare of the consumer minus his/her energy costs. The comfort level is formulated in detail in Section II-G. The consumers determine the comfort levels using their SHEMSs.

C. Model of SHEMSs

At the beginning of each day, each SHEMS participates in the utility company's pricing program to determine the optimal real-time electricity prices. Then, the SHEMS executes distributed

resilient DRP process considering the optimal real-time electricity prices and the system determines the initial schedule of power consumptions of home appliances and charging/discharging power of ESS.

D. Model of Smart Home Appliances

It is assumed that each consumer uses five smart appliances consist of: $d \in D = \{\text{AC}, \text{PHEV}, W, L, \text{Ent}\}$.

The smart appliances are air conditioning (AC) system, PHEV, washing-drying machine (W), lighting system (L), and entertainment system. The models of appliances are presented as the following formulations.

1) *Air Conditioning System*: The AC system controls the inside temperature of the consumer's house. $\text{Temp}_i^{\text{in}}(t)$ and $\text{Temp}_i^{\text{out}}(t)$ are the inside and outside temperatures of the consumer house. The inside temperature of the consumer house i at time t is determined by

$$\text{Temp}_i^{\text{in}}(t) = \text{Temp}_i^{\text{in}}(t-1) + \alpha(\text{Temp}_i^{\text{out}}(t) - \text{Temp}_i^{\text{in}}(t-1)) + \beta p_{i,\text{AC}}(t) \quad (1)$$

where α is the heat transfer between the indoor and outdoor environments of the house, and β is the thermal efficiency of the air conditioner. The negative value of β denotes that the air conditioner is a cooling system. $T_{i,\text{AC}}$ is a set of times that consumer i cares about the inside temperature of the home. There is a desired temperature range for each consumer $[\text{Temp}_i^{\text{conf,min}}, \text{Temp}_i^{\text{conf,max}}]$ and the indoor temperature should be within the following range:

$$\text{Temp}_i^{\text{conf,min}} \leq \text{Temp}_i^{\text{in}}(t) \leq \text{Temp}_i^{\text{conf,max}} \quad \forall i \in J. \quad (2)$$

Further, the preferred temperature for each consumer is defined by $\text{Temp}_i^{\text{conf}}$, which is determined by each consumer. Further, the air conditioning system can consume the maximum values of power $p_{i,\text{AC}}^{\text{max}}$. Thus

$$0 \leq p_{i,\text{AC}}(t) \leq p_{i,\text{AC}}^{\text{max}} \quad \forall t \in T \quad \forall i \in J. \quad (3)$$

For intervals that the consumers do not care about the temperature inside their home $T \setminus T_{i,\text{AC}}$

$$p_{i,\text{AC}}(t) = 0 \quad \forall t \in T \setminus T_{i,\text{AC}} \quad \forall i \in J. \quad (4)$$

The welfare that consumer i derives from using of the AC system can be written as a differentiable and concave function of $\text{Temp}_i^{\text{in}}(t)$

$$\text{Wel}_{i,\text{AC}} = a_{i,\text{AC}} - b_{i,\text{AC}}(\text{Temp}_i^{\text{in}}(t) - \text{Temp}_i^{\text{conf}})^2 \quad \forall i \in J \quad (5)$$

where $a_{i,\text{AC}}$ and $b_{i,\text{AC}}$ are positive constants that are selected by consumers based on their preferences. When the difference between the indoor temperature and the desired temperature increases, the consumer welfare, and consequently, consumer comfort decreases.

2) *PHEV*: The consumers only care about their PHEVs to be charged to a certain level within a specified time ($T_{i,\text{PHEV}}$).

There is a maximum charge power $p_{i,\text{PHEV}}^{\text{max}}$ for each PHEV

$$0 \leq p_{i,\text{PHEV}}(t) \leq p_{i,\text{PHEV}}^{\text{max}} \quad \forall t \in T_{i,\text{PHEV}} \quad \forall i \in J. \quad (6)$$

At times when electric cars are not at home $T \setminus T_{i,\text{PHEV}}$

$$p_{i,\text{PHEV}}(t) = 0 \quad \forall t \in T \setminus T_{i,\text{PHEV}} \quad \forall i \in J. \quad (7)$$

$E_{i,\text{PHEV}}^{\min}$ and $E_{i,\text{PHEV}}^{\max}$ denote the minimum and maximum values of total energy for charging of PHEV, respectively,

$$\begin{aligned} E_{i,\text{PHEV}}^{\min} &\leq \sum_{t \in T_{i,\text{PHEV}}} (\text{Eff}_{i,\text{PHEV}} p_{i,\text{PHEV}}(t)) \\ &\leq E_{i,\text{PHEV}}^{\max} \quad \forall i \in J \end{aligned} \quad (8)$$

where $\text{Eff}_{i,\text{PHEV}}$ determines the battery efficiency of each PHEV according to the energy losses and current leakage of the charging process. The total welfare that consumer i derives from charging the PHEV depends on the total stored energy of the vehicle and is defined as a differentiable and concave function of $E_{i,\text{PHEV}}$ as follows:

$$\text{Wel}_{i,\text{PHEV}}(E_{i,\text{PHEV}}) = a_{i,\text{PHEV}} E_{i,\text{PHEV}} + b_{i,\text{PHEV}} \quad (9)$$

where $a_{i,\text{PHEV}}$ and $b_{i,\text{PHEV}}$ are positive constants that the consumer adjusts according to his/her preferences. When the battery energy level of the PHEV at the end of the day increases, consumer welfare, and consequently, consumer comfort increases.

3) *Washing-Drying Machine*: It is assumed that the consumers maximize the cleanliness of their clothes as much as possible using the washing-drying machines. Therefore, the welfare of consumers increases as their clothes become cleaner. $T_{i,W}$ is the set of times that the consumer can use his/her washing-drying machine. The maximum value of power consumption for the washing-drying machine is formulated as

$$0 \leq p_{i,W}(t) \leq p_{i,W}^{\max} \quad \forall t \in T_{i,W} \quad \forall i \in J. \quad (10)$$

Further, when the consumers do not use their washing-drying machines $T \setminus T_{i,W}$, the value of power consumption can be written as

$$p_{i,W}(t) = 0 \quad \forall t \in T \setminus T_{i,W} \quad \forall i \in J. \quad (11)$$

The minimum and maximum values of washing-drying energy consumption are $E_{i,W}^{\min}$ and $E_{i,W}^{\max}$, respectively. Thus, the aggregated power consumption of washing-drying machine can be presented by

$$E_{i,W}^{\min} \leq \sum_{t \in T_{i,W}} p_{i,W}(t) \leq E_{i,W}^{\max} \quad \forall i \in J. \quad (12)$$

The total welfare that consumer i derives from using his/her washing-drying machine depends on the total energy that this appliance consumes. Thus, welfare can be defined as a differentiable and concave function of $E_{i,W}$ as follows:

$$\text{Wel}_{i,W}(E_{i,W}) = a_{i,W} E_{i,W} + b_{i,W} \quad (13)$$

where $a_{i,W}$ and $b_{i,W}$ are positive constants that consumer adjusts these parameters according to his/her preference. Based on the proposed formulation, the welfare of the consumer enhances as the energy consumption of the washing-drying machine increases and the consumer's clothes becomes cleaner.

4) *Lighting System*: It is assumed that the $T_{i,L}$ parameter indicates the hours that the consumer i keeps turning on his/her lighting system. The value of power consumption of the lighting

system to achieve the desired brightness is defined as $p_i^{\text{Light.comf}}$. Further, the maximum power consumption of the lighting system is defined as $p_{i,L}^{\max}$. Thus, the power consumption of lighting system can be written as

$$0 \leq p_{i,L}(t) \leq p_{i,L}^{\max} \quad \forall t \in T_{i,L} \quad \forall i \in J. \quad (14)$$

Hence, when the lighting system is turned off its power consumption can be presented as

$$p_{i,L}(t) = 0 \quad \forall t \in T \setminus T_{i,L} \quad \forall i \in J. \quad (15)$$

The consumer welfare that he/she derives from using his/her lighting system at time $t \in T_{i,L}$ is formulated as a differentiable and concave function of $p_{i,L}(t)$

$$\text{Wel}_{i,L}(p_{i,L}(t)) = a_{i,L} - b_{i,L}(p_{i,L}(t) - p_i^{\text{Light.comf}})^2 \quad (16)$$

where $a_{i,L}$ and $b_{i,L}$ are positive constants that the consumer adjusts according to his/her preferences. When the difference between the obtained and the desired brightness increases, the consumer welfare and comfort decrease.

5) *Entertainment System*: The entertainment system includes a TV, game console, and computer. The desired power consumption of the entertainment system is presented as $p_i^{\text{Ent.comf}}(t)$. It is assumed that the $T_{i,\text{Ent}}$ parameter indicates the hours that the consumer i keeps turning on his/her entertainment system. The maximum power consumption of the entertainment system is defined as $p_{i,\text{Ent}}^{\max}$. Thus, the power consumption of entertainment system can be written as

$$0 \leq p_{i,\text{Ent}}(t) \leq p_{i,\text{Ent}}^{\max} \quad \forall t \in T_{i,\text{Ent}} \quad \forall i \in J. \quad (17)$$

When the entertainment system is turned off, its power consumption can be presented as

$$p_{i,\text{Ent}}(t) = 0 \quad \forall t \in T \setminus T_{i,\text{Ent}} \quad \forall i \in J. \quad (18)$$

The consumer welfare that he/she derives from using his/her entertainment system at time $t \in T_{i,\text{Ent}}$ is formulated as a differentiable and concave function of $p_{i,\text{Ent}}(t)$

$$\begin{aligned} \text{Wel}_{i,\text{Ent}}(p_{i,\text{Ent}}(t)) &= a_{i,\text{Ent}} \\ &- b_{i,\text{Ent}}(p_{i,\text{Ent}}(t) - p_i^{\text{Ent.comf}}(t))^2 \end{aligned} \quad (19)$$

where $a_{i,\text{Ent}}$ and $b_{i,\text{Ent}}$ are positive constants that consumer adjusts them according to their preferences. When the difference between the obtained and the desired power consumption of the entertainment system increases, the consumer welfare and comfort decrease.

E. Model of ESS

The electrical energy storage facility is utilized to enhance the flexibility and resiliency of the system. The integration of ESS with the DRP enables the consumer to use his/her appliances in emergency conditions.

The ESS capacity energy level and state of charge (SOC) are denoted by Cap_i and $\text{soc}_i(t)$, respectively. Further, the charge and discharge powers are $p_i^{\text{chg}}(t)$ and $p_i^{\text{dchg}}(t)$, respectively.

The cost of ESS is presented by

$$B\text{Cost}_i(p_i^{\text{chg}}(t) + p_i^{\text{dchg}}(t)). \quad (20)$$

The SOC of the ESS is determined by

$$\text{soc}_i(t) = \sum_{\tau=1}^t (rt\text{Eff}_i \cdot p_i^{\text{chg}}(\tau) + p_i^{\text{dchg}}(\tau)) + \text{soc}_i(0) \quad (21)$$

where $\text{soc}_i(0)$ is the ESS SOC at the beginning of the simulation interval. $rt\text{Eff}$ denotes the round trip efficiency of each consumer's ESS. The maximum values of charging and discharging power are $p_i^{\text{chg,max}}$, $p_i^{\text{dchg,max}}$, respectively. Thus, the charging and discharging constraints can be written as

$$0 \leq p_i^{\text{chg}}(t) \leq p_i^{\text{chg,max}} \quad \forall t \in T \quad \forall i \in J \quad (22)$$

$$p_i^{\text{dchg,max}} \leq p_i^{\text{dchg}}(t) \leq 0 \quad \forall t \in T \quad \forall i \in J. \quad (23)$$

Further, the maximum value of soc is presented by

$$0 \leq \text{soc}_i(t) \leq \text{Cap}_i \quad \forall t \in T \quad \forall i \in J. \quad (24)$$

The cost function of electrical energy storage is defined as a convex function of $(p_i^{\text{chg}}(t) + p_i^{\text{dchg}}(t))$ that can be formulated as

$$\begin{aligned} & \text{BCost}_i(p_i^{\text{chg}}(t) + p_i^{\text{dchg}}(t)) \\ &= \sigma_1 \sum_{t \in T} (p_i^{\text{chg}}(t) + p_i^{\text{dchg}}(t))^2 \\ & - \sigma_2 \sum_{t=1}^{23} ((p_i^{\text{chg}}(t) + p_i^{\text{dchg}}(t))(p_i^{\text{chg}}(t+1) \\ & + p_i^{\text{dchg}}(t+1))) \\ & + \sigma_3 \sum_{t \in T} (\min(\text{soc}_i(t) - \gamma \text{Cap}_i, 0))^2 + \sigma_4 \end{aligned} \quad (25)$$

where, σ_1 , σ_2 , and σ_3 are positive constants. The first term of (25) presents the destructive effect of fast charging and discharging on the ESS. The second term denotes that if the values of $(p_i^{\text{chg}}(t) + p_i^{\text{dchg}}(t))$ and $(p_i^{\text{chg}}(t+1) + p_i^{\text{dchg}}(t+1))$ have different signs, an additional cost will be imposed. The third term presents that the available energy level of ESS should be greater than a predefined minimum value, which is denoted by γ . Finally, the fourth term (σ_4) is a function of the calendar life of the ESS.

F. Cost Function of the Utility Company

It is assumed that the cost function of the utility company can be presented as a quadratic function

$$\begin{aligned} & \text{Cost}(p(t)) \\ &= \begin{cases} cc_1(p(t))^2 + cb_1(p(t)) + ca_1; 0 \leq p(t) \leq X_1 \\ cc_2(p(t))^2 + cb_2(p(t)) + ca_2; X_1 \leq p(t) \leq X_2 \\ \vdots \\ cc_m(p(t))^2 + cb_m(p(t)) + ca_m; X_{m-1} \leq p(t) \leq X_m \end{cases} \end{aligned} \quad (26)$$

where $cc_m > cc_{m-1} > \dots > cc_1 > 0$.

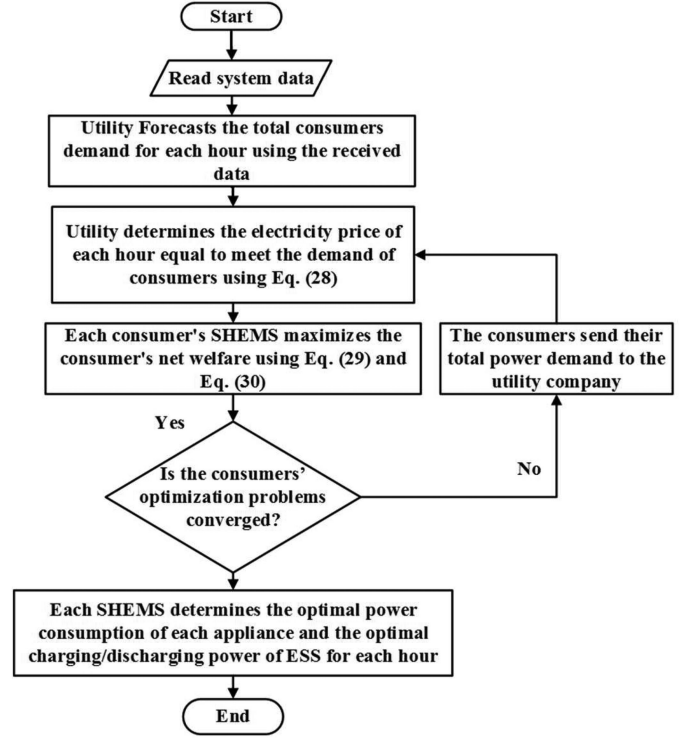


Fig. 1. Proposed algorithm flowchart.

G. Objective Function of Consumer

It is assumed that the consumer utilizes smart appliances to maximize his/her comfort level. Thus, the objective function of each consumer is defined as

$$\begin{aligned} \max \text{CL}_i = & \max \sum_{t \in T} \left(\sum_{d \in D} \text{wel}_{i,d}(p_{i,d}(t)) \right) \\ & - \text{BCost}_i(p_i^{\text{chg}}(t), p_i^{\text{dchg}}(t)) - \sum_{t \in T} \text{Pr}(t)p_i(t) \end{aligned} \quad (27)$$

where $\text{Pr}(t)$ is the electricity price at time t .

III. SOLUTION ALGORITHM OF DYNAMIC REAL-TIME PRICING AND DRP

As shown in Fig. 1, at first, the utility company performs an hourly demand forecast $p(t) \quad \forall t \in T$. Then, the utility company determines the electricity price of each hour to meet the demand of consumers based on

$$\text{Pr}^n(t) = \text{cost}' \left(\sum_i^n p_i^{n-1}(t) \right) \quad \forall t \in T \quad (28)$$

where $p_i^{n-1}(t)$ is the optimal power consumption of consumer i at time t in the $(n-1)$ th iteration of the algorithm. The $p_i^{n-1}(t)$ is determined by the SHEMS of the consumer i to maximize his/her welfare. Further, $\text{Pr}^n(t)$ presents the electricity price at time t in the n th iteration of the algorithm.

The SHEMS calculates the optimal values of power consumption of consumer appliances and charging /discharging power of

ESS by solving the following equations, respectively,

$$p_{i,d}^n(t) = p_{i,d}^{n-1}(t) + \gamma \left(\frac{\partial \text{Wel}_{i,d}(p_{i,d}^{n-1}(t))}{\partial p_{i,d}^{n-1}(t)} - \text{Pr}^n(t) \right) \quad \forall t \in T_{i,d} \quad \forall i \in J \quad \forall d \in D \quad (29)$$

$$(p_i^{\text{chg},n}(t) + p_i^{\text{dchg},n}(t)) = (p_i^{\text{chg},n-1}(t) + p_i^{\text{dchg},n-1}(t)) - \gamma \left(\frac{\partial \text{BCost}_i(p_i^{\text{chg},n-1}(t) + p_i^{\text{dchg},n-1}(t))}{\partial (p_i^{\text{chg},n-1}(t) + p_i^{\text{dchg},n-1}(t))} + \text{Pr}^n(t) \right) \quad \forall t \in T \quad \forall i \in J \quad (30)$$

where $p_{i,d}^n(t)$ is the power consumption of appliance d of the consumer i at time t and at the n th iteration of the algorithm. Further, $p_i^{\text{chg},n}(t)$ and $p_i^{\text{dchg},n}(t)$ are the values of charging and discharging power of the ESS of the consumer i at time t and at the n th iteration of the algorithm, respectively. γ is a constant step size. Then, the consumer reports his/her total power demand $p_i^n(t) \quad \forall t \in T \quad \forall i \in J$ to the utility company through smart meter infrastructure. This optimization process is repeated until convergence is achieved.

The main advantages of the proposed algorithm are: the utility company does not need to have the detailed information of the consumers' consumption and the hourly data of total consumption of consumer is adequate for simulating process; the hourly data of total consumption of consumer is more accurate than the previous information of the consumer's consumption; and the utility company does not have to solve complex equations to determine the optimal prices.

IV. SIMULATION INPUT DATA

In this article, at the first step, 20 households were simulated in a neighborhood in the Southern California area. Based on [32], [33] data, there were 5.07 persons per household (PPH) for the 2009 year in the selected area. Further, the annual population growth rate was about 0.61% [32].

Thus, it was assumed that each of these households comprised six people for 2021 considering the population growth rate. Then, the sensitivity analysis for the number of households and number of PPH was performed. The simulation was carried out for a typical summer day. Based on the International Energy Conservation Code (IECC) climate zones, as shown in Fig. 2, the United States is divided into eight different climatic zones and the California state is located in the third zone. The hourly outside temperature $\text{Temp}_i^{\text{out}}(t)$ for a typical summer day is shown in Fig. 3. The households were divided into two categories: The first group of households are $J1 = \{i_1, i_2, i_3, \dots, i_{10}\}$ that the families were at home all day. The second group are $J2 = \{i_{11}, i_{12}, i_{13}, \dots, i_{20}\}$, which the families were not at home for 08:00–18:00 h. It was assumed that the area of each house was 250 square meters and all the houses were single-level buildings with a concrete slab floor, which removed up to 215.2 BTU of heat for every square meter of floor area. Thus, for each house, it was considered that an air conditioning system with a capacity of 53800 BTU was needed and each household used the American Standard Platinum 20 Series TAM 9 model

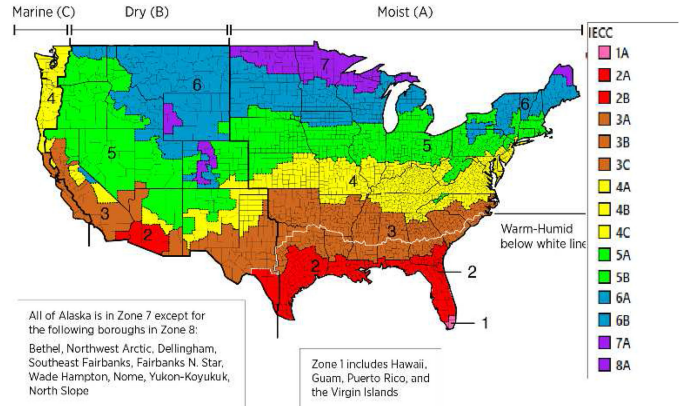


Fig. 2. IECC climate zones map [34].

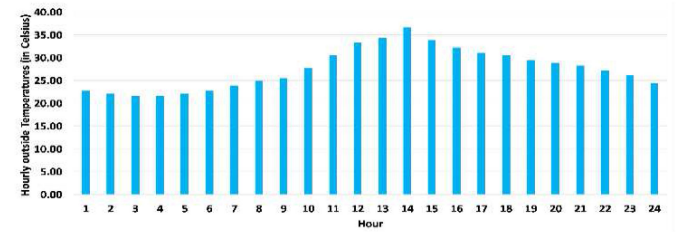


Fig. 3. Hourly temperature outside of the simulated houses [35].

TABLE I
COEFFICIENTS OF THE WELFARE FUNCTIONS

$a_{i,AC} = 3.45$	$b_{i,AC} = 0.06$	$a_{i,PHEV} = 0.0009$	$b_{i,PHEV} = 0.3$	$a_{i,W} = 0.002$
$b_{i,W} = 0.466$	$a_{i,L} = 0.76$	$b_{i,L} = 0.06$	$a_{i,Ent} = 0.3$	$b_{i,Ent} = 0.03$

4A7V0060A1 central air conditioning system with the capacity of 54000 BTU and the energy efficiency ratio of 12.75.

It was assumed that the air conditioning system was determined as the first rank of the consumers' priority list based on the fact that the simulation was run for a typical summer day. Then, the PHEV and washing-drying machine were chosen as the second and third ranks of the list. Finally, the last priorities were the lighting system and the entertainment system. Therefore, the coefficients of the welfare functions for different appliances were selected as given in Table I. Table II gives the input data for the simulation of smart home appliances and ESS. The desired amount of power consumption for the entertainment system is given in Table III. As shown in Fig. 4, the 18-bus IEEE test system was considered as a part of the utility that the smart homes were allocated. The priority list numbers were determined by the consumers. The more importance was given to the home appliance that was the higher priority for that consumer in normal and emergency conditions.

V. SIMULATION RESULTS

The simulation was carried out using GAMS optimization software version 25.1.3 and MATLAB (MATPOWER for OPF) on a computer system with Intel Core i7-5500 U CPU @ 2.40 GHz 2.40 GHz processor and 8 GB of memory. The simulation time for 20 households was about 19 s.

TABLE II
DATA FOR THE SIMULATION OF THE SMART HOME APPLIANCES AND ESS

Preferred household temperature (Celsius)					
$Temp^{conf}$	23.89°	$Temp^{conf,max}$	25°	$Temp^{conf,min}$	21.11°
Household PHEV					
Capacity	12 kWh		P_{PHEV}^{max}	3.7 kW	
E_{PHEV}^{max}	10.4 kWh		E_{PHEV}^{min}	9.88 kWh	
Household washer-dryer (1500 RPM, 8.5 kg)					
E_W^{max}	5.44 kWh	E_W^{min}	5.3 kWh	P_W^{max}	2.2 kW
Controllable LED lights (45 W LED, 5800 lumens)					
p_L^{max}	580 W	p_{light}^{conf}	435 W	$T_{i,L} = \{19, 20, \dots, 24\}$	
TV (85" QLED 8K UHD HDR Smart TV)					
TV ave. power	255 W		TV max. power	585 W	
5.1-Channel Home Theatre System					
ave. power	275 W		max. power	580 W	
Game Console					
ave. power	158.2 W		max. power	310 W	
Computer					
ave. power	185 W		max. power	295 W	
ESS					
Cap	13.5 kWh	$p^{chg,max}$	5 kW	$rtEff$	90%
η	0.3		γ	0.2	

TABLE III
CONSUMERS' DESIRED TIME OF USING EACH DEVICE FOR THE ENTERTAINMENT SYSTEM

	Household category	Active hours	Standby hours	Off hours
TV	1	10→12, 18→20, 21→24	8→10, 12→18, 20→21	0→8
	2	19→20, 21→24	18→19, 20→21	0→18
Home Theater	1	10→12, 18→20, 21→24	8→10, 12→18, 20→21	0→8
	2	19→20, 21→24	18→19, 20→21	0→18
Game Console	1	18→20	8→18, 20→24	0→8
	2	19→20	18→19, 20→24	0→18
Computer	1	8→12, 13→15	-	0→8, 12→13, 15→24
	2	18→19	-	0→18, 19→24

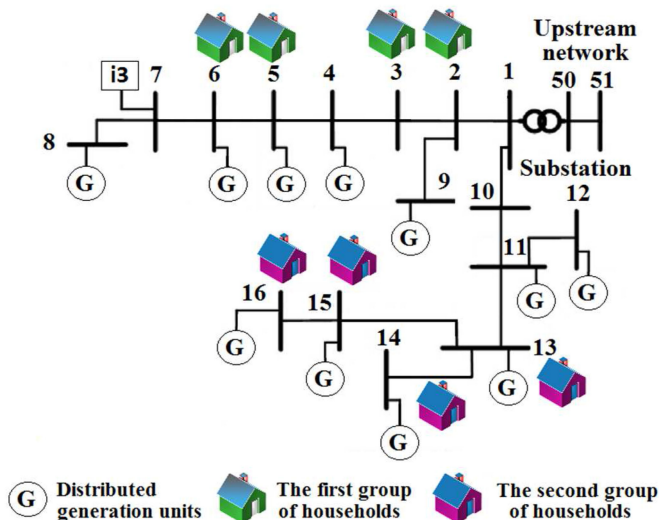


Fig. 4. 18-bus IEEE test system topology.

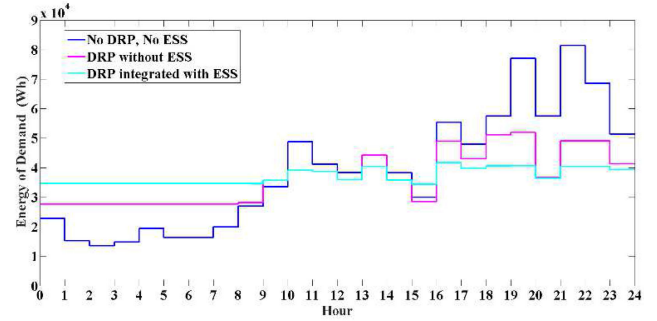


Fig. 5. Demand of energy of consumers for different steps under normal operating conditions.

TABLE IV
RESULTS OF THE LOWEST, HIGHEST, AND AVERAGE PRICES OF ELECTRICITY CASES FOR NORMAL OPERATING CONDITIONS

	Real time price (\$/kWh)		
	Min	Max	Avg.
No DRP, No ESS	13.813 ($t : 2 \rightarrow 3$)	111.119 ($t : 21 \rightarrow 22$)	37.924
DRP without ESS	26.291 ($t : 0 \rightarrow 8$)	47.837 ($t : 19 \rightarrow 20$)	34.239
DRP and ESS	32.195 ($t : 15 \rightarrow 16$)	38.674 ($t : 16 \rightarrow 17$)	34.698

A. Normal Operation Conditions

Under these operating conditions, the proposed model was initially simulated without DRP/ESS and the consumers maximized their welfare regardless of electricity prices. In the next case, the DRPs were applied and the consumers reacted to real-time electricity prices through the DRP. In the final case of normal operation conditions, the DRPs with the home ESSs were integrated. Thus, three cases were considered for the normal operation conditions.

- 1) Case 1: The DRP and ESS were not considered.
- 2) Case 2: The DRP without ESS was considered.
- 3) Case 3: The DRP was integrated with ESS.

Fig. 5 shows the total demand of energy of consumers for different cases of simulation under normal operating conditions. As shown in Fig. 5, the proposed DRP significantly reduced the peak of demand and effectively flattened the load shape. Table IV gives the results of the lowest, highest, and average prices of electricity cases for normal operating conditions. Table V gives a brief comparison of three cases of the normal operating conditions. According to Table V, the real-time pricing method effectively increased the load factor. The proposed method not only reduced the energy purchased cost for the utility company but also increased the comfort level of the consumers.

Besides, the integration of ESS with the DRP increased the comfort level of each consumer and the load factor of the system. It also effectively reduced the cost of the utility company and the energy cost of consumers. For the third case, the total energy demand of consumers' increased, but the energy purchased costs

TABLE V
BRIEF COMPARISON FOR THREE CASES OF THE NORMAL
OPERATING CONDITIONS

	No DRP, No ESS	DRP without ESS	DRP and ESS
Load Factor (LF)	0.479	0.704	0.892
Peak Demand (PD) (kWh)	81.421	51.974	41.621
Total Demand (TD) (kWh)	936.496	878.610	891.076
Cost Of Utility (COU) (\$)	278.072	209.105	206.037
Total Payment Of Consumers (TPOC) (\$)	455.215	317.025	310.661
Welfare Of Consumers (WOC) (\$)	1370.617	1347.570	1351.963
Operational Costs Of ESS (OCOESS) (\$)	0	0	1.594
Total Comfort Level Of Consumers (TCLOC) (\$)	915.402	1030.545	1039.709
Social Welfare (SW) (\$)	1092.546	1138.466	1144.332

of the utility and consumers were reduced. Further, for the third case, the welfare of consumers was increased.

B. Emergency Operating Conditions

For emergency operating conditions, sixty-nine scenarios were considered to model the power supply disruptions every 24 h of the day

$$S = \{s_{1,1}, s_{1,2}, s_{1,3}, s_{2,1}, s_{2,2}, s_{2,3}, \dots, s_{23,1}, s_{23,2}, s_{24,1}\}.$$

For example, $s_{22,3}$ presents the scenario that the power supply disruption occurred for the twenty-second hour of the day (from 21:00 to 22:00) and lasted for three hours. The set of times when the power supply was disconnected is presented: $T_s \forall s \in S$ for each scenario.

The following conditions were considered to model the emergency conditions.

- 1) The ESS charging power was zero during the hours when the power supply from the network to consumers was disconnected

$$p_i^{\text{chg}}(t) = 0 \forall t \in T_s \forall i \in J. \quad (31)$$

- 2) When the utility power supply disconnected, the power consumption of the household appliances equaled to the discharge power of the household ESS

$$p_i^{\text{dchg}}(t) + \sum_{d \in D} p_{i,d}(t) = 0 \forall t \in T_s \forall i \in J. \quad (32)$$

The System Average Interruption Duration Index (SAIDI) for these emergency conditions was considered two hours according to [36]. The SAIDI values for less destructive and more destructive emergency cases were considered one hour and three hours, respectively. Numerous emergency scenarios were generated and their impacts on the utility system and consumers were analyzed.

The worst-case emergency scenarios are as follows.

- 1) *Worst-Case Scenario 1*: Supply interruption for 11:00–14:00.

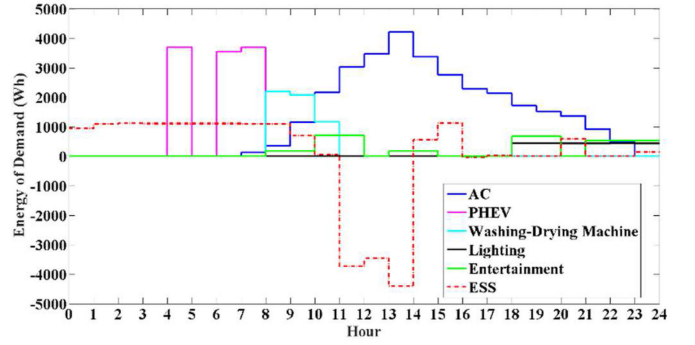


Fig. 6. Demand of energy of the first category of consumers' household for the worst-case scenario 1.

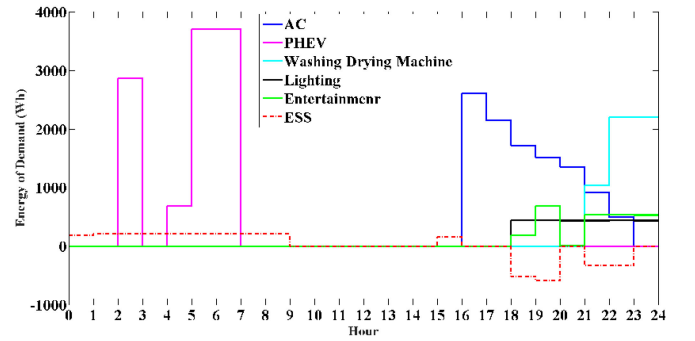


Fig. 7. Demand of energy of the second category of consumers' household for the worst-case scenario 1.

- 2) *Worst-Case Scenario 2*: Supply interruption for 16:00–19:00.

Figs. 6 and 7 show the demand of energy of the first and second categories of households for the worst-case scenario 1, respectively. As shown in Fig. 6, the power supply interruption occurred between 11:00 and 14:00 h, when the consumer was at home. Despite the high power consumption of the AC system, the proposed DRP committed the EES to increase the comfort level of the consumer that utilized his/her entertainment system. According to Fig. 7, the power supply interruption occurred when the consumer was not at home. Therefore, the power outage did not affect the second type of residential consumers. However, due to the large difference between the outdoor temperature and the desired temperature, the power consumption of the AC system was high. Thus, this scenario was known as the worst-case emergency scenario. Fig. 8 depicts the aggregated demand of energy of the first and second categories of households for the worst-case scenario 1. As shown in Fig. 8, due to the interruption of power supply, the aggregated demand of energy of consumers was zero for 11:00–14:00, but the air conditioning and entertainment systems were active.

In this emergency condition, the ESS supplied other appliances of consumers. Despite the high electrical energy consumption of the air conditioning system, consumers utilized their entertainment system during emergency condition hours.

Figs. 9 and 10 present the demand of energy of the first and second categories of households for the worst-case scenario 2, respectively. As shown in Fig. 9, the power supply interruption

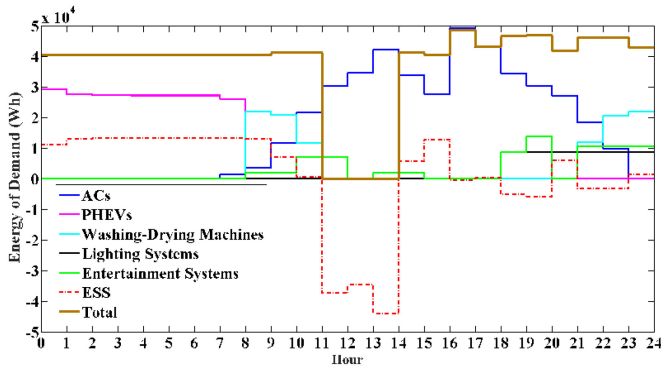


Fig. 8. Aggregated demand of energy of the consumers' household for the worst-case scenario 1.

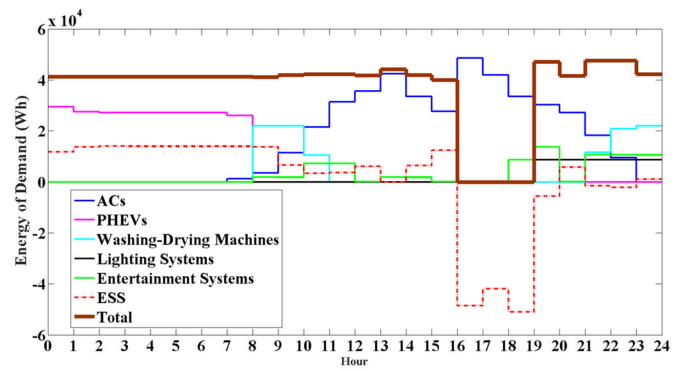


Fig. 11. Aggregated demand of energy of the consumers' household for the worst-case scenario 2.

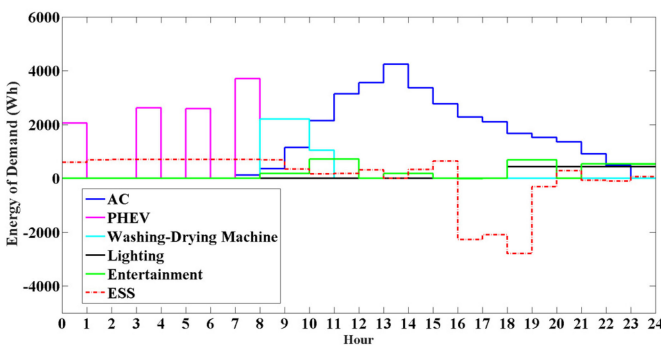


Fig. 9. Demand of energy of the first category of consumers' household for the worst-case scenario 2.

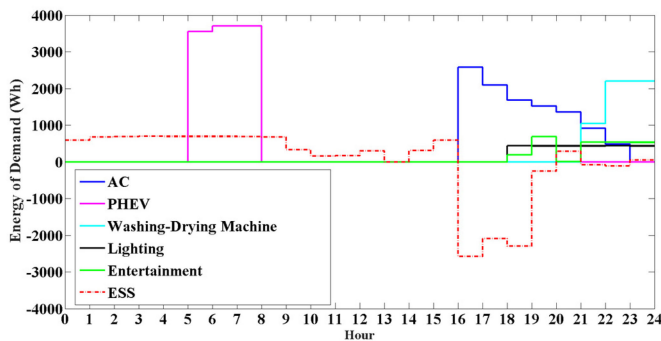


Fig. 10. Demand of energy of the second category of consumers' household for the worst-case scenario 2.

occurred between 16:00 and 19:00 h for the second scenario. The ESS supplied the consumer's power demand. By comparing this scenario and the first worst-case scenario, it can be concluded that the AC system energy consumption was decreased. According to Fig. 10, when the power supply interruption occurred, the consumer was not at home from 16:00 to 18:00 h. However, the difference between the indoor temperature and the consumer's desired temperature was high base on the fact that the AC system was off before 16:00 h. Thus, the AC system energy consumption was high and this scenario was one of the worst-case scenarios. Gradually, as the indoor temperature decreased between 18:00 and 19:00 h, the AC consumption decreased, and the consumer

used the lighting system and entertainment system by using the proposed DRP integrated with ESS.

Fig. 11 depicts the aggregated demand of energy of the first and second categories of households for the worst-case scenario 2. By comparing Figs. 8 and 11, it can be concluded that the proposed model optimized the DRP process with no load shedding or curtailment, which did not reduce the comfort level of the consumers.

Thus, the proposed model considered both the priority and the desired comfort level of the consumers, not only for normal operating conditions but also in emergency operating conditions. It is important to note that despite an emergency condition that had disconnected the power delivery to the consumers, the proposed model successfully supplied the consumers and they utilized their home appliances. The results showed that the proposed DRP integrated with the ESS using the real-time pricing method controlled the demand and flattened the load shape of the consumers.

C. Sensitivity Analysis

A sensitivity analysis was carried out to assess the impacts of the number of households on the simulation process outputs. For the sensitivity analysis, the number of households was considered 20, 50, and 100, respectively. Further, for each of these scenarios, the number of PPH was assumed three and six. For the three PPH case, the simulation input data were readjusted. Thus, the AC system and electricity consumption of home appliances were reduced. Hence, the worst-case scenario was the supply interruption from 21:00 to 24:00 for this case.

As given in Table VI and for three PPH, when the number of households increased, the load factor, peak load, and the total load increased. The costs of utility for normal conditions were decreased by about 14.09% and 29.84% for 20 and 100 households, respectively. The total payments of consumers for normal conditions were decreased by about 19.37% and 30.49% for 20 and 100 households, respectively.

Further, the consumers comfort level for normal conditions increased by about 3.32% and 78.64% for 20 and 100 households,

TABLE VI
COMPARISON BETWEEN THE NORMAL OPERATION MODE, WORST-CASE SCENARIOS, AND THE AVERAGE VALUES OF VARIABLES IN EMERGENCY CONDITIONS

PPH		6			3		
Households		20	50	100	20	50	100
I.F	A1	0.47	0.5	0.49	0.47	0.46	0.47
	A2	0.89	0.92	0.93	0.9	0.92	0.92
	A3	0.44	0.48	0.48	0.7	0.45	0.45
	A4	0.82	0.84	0.84	0.836	0.85	0.85
	A5	0.76	0.79	0.79			
	B5				0.78	0.79	0.79
PD (kWh)	A1	81.42	196.56	396.75	65.3	168.65	330.35
	A2	41.62	96.92	188.62	33.66	79.95	151.98
	A3	74.88	201.75	404.84	43.14	171.89	345.68
	A4	45.01	105.88	208.18	37.18	86.21	165.17
	A5	48.64	133.92	222.65			
	B5				39.25	91.01	174.37
TD (kWh)	A1	936.49	2341.24	4682.47	738.69	1846.73	3693.45
	A2	891.07	2135.98	4206.12	726.89	1760.29	3371.02
	A3	905.95	2341.24	4682.47	720.59	1846.73	3693.45
	A4	887.76	2128.3	4189.27	725.67	1753.51	3372.21
	A5	889.7	2155.96	4244.97			
	B5				733.69	1772.89	3409.48
COU (\$)	A1	278.07	1336.67	5120.84	178.9	836.83	3142.32
	A2	206.03	926.02	3391.55	153.69	647.76	2204.7
	A3	269.76	1398.78	5410.93	162.67	895.85	3418.98
	A4	214.5	1012.68	3737.85	160.32	705.54	2448.85
	A5	221.02	1058.98	3921.7			
	B5				164.27	722.92	2509.19
TPOC (\$)	A1	455.21	2545.24	10070.5	259.19	1554.66	6131.664
	A2	310.66	1727.73	6620.69	208.99	1178.12	4262.36
	A3	445.48	2678.32	10659.55	235.91	1681.55	6693.84
	A4	334.63	1910.04	7322.46	231.13	1302.65	4759.5
	A5	351.29	2003.9	7690.9			
	B5				240.65	1356.3	4955.54
WOC (\$)	A1	1370.61	3998.54	7997.09	1599.42	3998.543	7997.09
	A2	1351.96	3865.79	7599.53	1594.65	3932.2	7599.56
	A3	1234.7	3998.54	7997.09	1593.54	3998.543	7997.09
	A4	1348.03	3865.8	7599.52	1593.86	3920.66	7599.55
	A5	1344.49	3865.79	7599.51			
	B5				1585.36	3899.75	7559.02
OCOESS (\$)	A1	0	0	0	0	0	0
	A2	1.59	3.88	8.71	0.94	2.36	4.85
	A3	0	0	0	0	0	0
	A4	4.61	4.86	5.37	0.95	2.47	4.93
	A5	11.77	28.97	58.85			
	B5				7.373	19.16	38.25
TCLOC (\$)	A1	915.4	1453.31	-2073.42	1340.23	2443.88	1865.42
	A2	1039.7	2134.19	970.13	1384.72	2751.72	3332.35
	A3	789.22	1320.23	-2662.46	1357.63	2316.99	1303.25
	A4	1007.87	1950.9	271.689	1361.79	2615.54	2835.13
	A5	981.42	1832.93	-150.23			
	B5				1344.71	2524.29	2565.23
SW (\$)	A1	1092.54	2661.88	2876.25	1420.52	3161.71	4854.766
	A2	1144.33	2935.89	4199.27	1440.02	3282.08	5390.01
	A3	964.83	2599.77	2586.15	1430.88	3102.7	4578.11
	A4	1128.91	2848.26	3854.8	1432.59	3212.65	5145.78
	A5	1111.69	2777.84	3618.96			
	B5				1421.08	3157.67	5011.58
A6	1114.16	2780.2	3638.37				

A1: Normal operation mode without proposed method for 3 pph and 6 pph

A2: Normal operation mode using proposed method for 3 pph and 6 pph

A3: Average emergency operation mode without proposed method for 3 pph and 6 pph

A4: Average emergency operation mode for proposed method for 3 pph and 6 pph

A5: The first worst case scenario: Supply interruption for 11:00-14:00 for 6 pph case

B5: The worst case scenario: Supply interruption for 21:00-24:00 for 3 pph case

A6: The second worst case scenario: Supply interruption for 16:00-19:00 for 6 pph case

respectively. Finally, the social welfare for normal conditions increased by about 1.37% and 11.03% for 20 and 100 households, respectively.

By comparing the values of Table VI for the three PPH and 20 and 100 households, it can be concluded that the costs of utility for emergency conditions were decreased by about 1.44% and 30.81% for 20 and 100 households, respectively. The total payments of consumers for emergency conditions were decreased by about 2.03% and 28.90% for 20 and 100 households, respectively. Further, the consumers comfort level for emergency conditions increased by about 0.31% and 117.54% for 20 and 100 households, respectively.

Finally, the social welfare for emergency conditions increased by about 0.12% and 12.40% for 20 and 100 households, respectively. By comparing the values of Table VI for 6 PPH and 100 households, it can be concluded that the costs of utility in normal and emergency conditions were decreased by about 33.77% and 30.92%, respectively. The total payments of consumers in normal and emergency conditions were decreased by about 34.26% and 31.31%, respectively. Further, the consumers comfort level for normal and emergency conditions increased by about 146.78% and 110.2%, respectively. Finally, the social welfare for normal and emergency conditions increased by about 46% and 49.06%, respectively.

VI. CONCLUSION

This article presented a resilient distributed demand response process that was integrated with electrical storage systems in the SHEMS. The results for 100 households with six PPH in normal operating conditions can be presented as the comfort level of the consumers was increased by about 146.78%; meanwhile, the energy procurement costs of consumers were reduced by about 34.26%; the social welfare was increased by about 46%; and the utility costs from wholesale were reduced by about 33.77%. The proposed model results for 100 households with six PPH in the case of emergency operating conditions can be presented as the consumers were immediately supplied after a power outage; based on the priority and the desired comfort level of each consumer, the load commitment was performed; there was no load shedding or curtailment process in the emergency conditions; the utility cost was reduced by about 30.92%; the consumers' comfort level was increased by about 110.2%; the social welfare was increased by about 49.06%; and the value of total payments of consumers was decreased by about 31.31%. It can be concluded that the proposed model successfully improved the load factor of the distribution system and enhanced the resiliency of smart homes. The costs of the utility company and total payments of consumers were highly reduced in normal and emergency conditions. The method had better performance for the higher number of PPH and the social welfare and consumer comfort levels were increased for the higher number of PPH. Finally, the comfort levels of consumers were highly increased in the normal and emergency conditions. The authors are working on the DER commitment process that can be optimally dispatched through the proposed model as future work.

REFERENCES

- [1] H. Mehrjerdi, "Resilience oriented vehicle-to-home operation based on battery swapping mechanism," *Energy*, vol. 218, 2021, Art. no. 119528.
- [2] H. T. Dinh and D. Kim, "An optimal energy-saving home energy management supporting user comfort and electricity selling with different prices," *IEEE Access*, vol. 9, pp. 9235–9249, Jan. 2021, doi: [10.1109/ACCESS.2021.3050757](https://doi.org/10.1109/ACCESS.2021.3050757).
- [3] E. Chatterji and M. D. Bazilian, "Battery storage for resilient homes," *IEEE Access*, vol. 8, pp. 184497–184511, 2020.
- [4] H. Mehrjerdi, "Resilience-robustness improvement by adaptable operating pattern for electric vehicles in complementary solar-vehicle management," *J. Energy Storage*, vol. 37, 2021, Art. no. 102454.
- [5] A. Abessi and S. Jadid, "Internal combustion engine as a new source for enhancing distribution system resilience," *J. Modern Power Syst. Clean Energy*, vol. 9, no. 5, pp. 1130–1136, Sep. 2021.
- [6] K. Rahimi and M. Davoudi, "Electric vehicles for improving resilience of distribution systems," *Sustain. Cities Soc.*, vol. 36, pp. 246–256, 2018.
- [7] G. Razeghi, J. Lee, and S. Samuelsen, "Resiliency impacts of plug-in electric vehicles in a smart grid," Inst. Transp. Stud., Univ. California, Irvine, Report No.: UC-ITS-2020-64, Jan. 2021. Accessed: Sep. 23, 2021. [Online]. Available: <https://escholarship.org/uc/item/4j19d5p1>
- [8] N. Z. Xu and C. Y. Chung, "Reliability evaluation of distribution systems including vehicle-to-home and vehicle-to-grid," *IEEE Trans. Power Syst.*, vol. 31, no. 1, pp. 759–768, Jan. 2016.
- [9] P. Srikantha and D. Kundur, "Resilient distributed real-time demand response via population games," *IEEE Trans. Smart Grid*, vol. 8, no. 6, pp. 2532–2543, Nov. 2017.
- [10] B. Balasubramaniam, P. Saraf, R. Hadidi, and E. B. Makram, "Energy management system for enhanced resiliency of microgrids during islanded operation," *Elect. Power Syst. Res.*, vol. 137, pp. 133–141, 2016.
- [11] R. Nourollahi, P. Salayani, K. Zare, and B. Mohammadi Ivatloo, "Resiliency-oriented optimal scheduling of microgrids the presence of demand response programs using a hybrid stochastic robust optimization approach," *Int. J. Elect. Power Energy Syst.*, vol. 128, 2021, Art. no. 106723.
- [12] X. Liu, M. Shahidehpour, Z. Li, X. Liu, Y. Cao, and Z. Bie, "Microgrids for enhancing the power grid resilience in extreme conditions," *IEEE Trans. Smart Grid*, vol. 8, no. 2, pp. 589–597, 2016.
- [13] J. Aghaei, M. I. Alizadeh, P. Siano, and A. Heidari, "Contribution of emergency demand response programs in power system reliability," *Energy*, vol. 103, pp. 688–696, 2016.
- [14] K. Samarakoon, J. Ekanayake, and N. Jenkins, "Investigation of domestic load control to provide primary frequency response using smart meters," *IEEE Trans. Smart Grid*, vol. 3, no. 1, pp. 282–292, Mar. 2011.
- [15] J. A. Short, D. G. Infield, and L. L. Freris, "Stabilization of grid frequency through dynamic demand control," *IEEE Trans. Power Syst.*, vol. 22, no. 3, pp. 1284–1293, Aug. 2007.
- [16] R. Yu, W. Yang, and S. Rahardja, "A statistical demand-price model with its application in optimal real-time price," *IEEE Trans. Smart Grid*, vol. 3, no. 4, pp. 1734–1742, Dec. 2012.
- [17] N. Lu and Y. Zhang, "Design considerations of a centralized load controller using thermostatically controlled appliances for continuous regulation reserves," *IEEE Trans. Smart Grid*, vol. 4, no. 2, pp. 914–921, Jun. 2012.
- [18] C. Vivekananthan and Y. Mishra, "Stochastic ranking method for thermostatically controllable appliances to provide regulation services," *IEEE Trans. Power Syst.*, vol. 30, no. 4, pp. 1987–1996, Jul. 2014.
- [19] E. Rosales-Asensio, M. de Simón-Martín, D. Borge-Diez, J. J. Blanes-Peiró, and A. Colmenar-Santos, "Microgrids with energy storage systems as a means to increase power resilience: An application to office buildings," *Energy*, vol. 172, pp. 1005–1015, 2019.
- [20] H. Mehrjerdi and R. Hemmati, "Coordination of vehicle-to-home and renewable capacity resources for energy management in resilience and self-healing building," *Renewable Energy*, vol. 146, pp. 568–579, 2020.
- [21] M. Vahedipour-Dahraie, H. Rashidizadeh-Kermani, A. Anvari-Moghaddam, and J. M. Guerrero, "Stochastic risk-constrained scheduling of renewable-powered autonomous microgrids with demand response actions: Reliability and economic implications," *IEEE Trans. Ind. Appl.*, vol. 56, no. 2, pp. 1882–1895, Mar./Apr. 2020.
- [22] M. Vahedipour-Dahraie, H. Rashidizadeh-Kermani, and A. Anvari-Moghaddam, "Risk-based stochastic scheduling of resilient microgrids considering demand response programs," *IEEE Syst. J.*, vol. 15, no. 1, pp. 971–980, Mar. 2021.
- [23] M. W. Tian and P. Talebizadehsardari, "Energy cost and efficiency analysis of building resilience against power outage by shared parking station for electric vehicles and demand response program," *Energy*, vol. 215, 2021, Art. no. 119058.
- [24] H. Mehrjerdi, M. Saad, and S. Lefebvre, "Efficiency-resilience nexus in building energy management under disruptions and events," *IEEE Syst. J.*, pp. 1–10, Sept. 2020, doi: [10.1109/JSYST.2020.3021697](https://doi.org/10.1109/JSYST.2020.3021697).
- [25] N. Gaikwad, N. S. Raman, and P. Barooah, "Smart home energy management system for power system resiliency," in *Proc. IEEE Conf. Control Technol. Appl.*, Aug. 2020, pp. 1072–1079.
- [26] C. Gouveia, J. Moreira, C. L. Moreira, and J. P. Lopes, "Coordinating storage and demand response for microgrid emergency operation," *IEEE Trans. Smart Grid*, vol. 4, no. 4, pp. 1898–1908, Dec. 2013.
- [27] Z. Guo, G. Li, M. Zhou, and W. Feng, "Resilient configuration approach of integrated community energy system considering integrated demand response under uncertainty," *IEEE Access*, vol. 7, pp. 87513–87533, Jun. 2019, doi: [10.1109/ACCESS.2019.2924828](https://doi.org/10.1109/ACCESS.2019.2924828).
- [28] F. Hafiz, B. Chen, C. Chen, A. R. de Queiroz, and I. Husain, "Utilising demand response for distribution service restoration to achieve grid resiliency against natural disasters," *IET Gener., Transmiss. Distrib.*, vol. 13, no. 14, pp. 2942–2950, 2019.
- [29] A. Eseye, M. Lehtonen, T. Tukia, S. Uimonen, and R. Millar, "Optimal energy trading for renewable energy integrated building microgrids containing electric vehicles and energy storage batteries," *IEEE Access*, vol. 7, pp. 106092–106101, Aug. 2019, doi: [10.1109/ACCESS.2019.2932461](https://doi.org/10.1109/ACCESS.2019.2932461).
- [30] M. Vahedipour-Dahraie, A. Anvari-Moghaddam, and J. M. Guerrero, "Evaluation of reliability in risk-constrained scheduling of autonomous microgrids with demand response and renewable resources," *IET Renewable Power Gener.*, vol. 12, no. 6, pp. 657–667, 2018.
- [31] A. Gholami, T. Shekari, F. Aminifar, and M. Shahidehpour, "Microgrid scheduling with uncertainty: The quest for resilience," *IEEE Trans. Smart Grid*, vol. 7, no. 6, pp. 2849–2858, Nov. 2016.
- [32] "Census bureau quickfacts," 2019. Accessed: Aug. 24, 2021. [Online]. Available: <https://www.census.gov/quickfacts/fact/table/southsanjosehillscdp/california/PST04021>
- [33] C. Nagengest, *Almanac of American Demographic*, Bloomington, IN, USA: AuthorHouse, 2009.
- [34] International Code Council, Inc., "2012 International Energy Conservation Code," ISBN: 978-1-60983-058-8, Dec. 2012. Accessed: Sep. 23, 2021. [Online]. Available: <https://codes.iccsafe.org/content/IECC2012>
- [35] Cedar Lake Ventures, Inc., "Climate and Average Weather Year Round in South San Jose Hills, California, United States.," Average Hourly Temperature in the Summer in South San Jose Hills. Accessed: Sep. 23, 2021. [Online]. Available: <https://weatherspark.com/y/1971/Average-Weather-in-South-San-Jose-Hills-California-United-States-Year-Round#Sections-Temperature>.
- [36] The U.S. Energy Information Administration - (EIA), "Annual electric power industry report, form EIA-861 detailed data files," Dec. 2021. Accessed: Sep. 23, 2021. [Online]. Available: <https://www.eia.gov/electricity/data/eia861/>